Automatic Regions-of- Interest Selection based on Pearson's Correlation Coefficient

Arthur de Miranda Neto, Alessandro Correa Victorino, Isabelle Fantoni, Douglas Eduardo Zampieri

Automatic Regions-of-Interest Selection based on Pearson's Correlation Coefficient

A. Miranda Neto, A. Corrêa Victorino, I. Fantoni and D. E. Zampieri

***Abstract*—Navigation of a Mobile Robot is based on its interaction with the environment, through information acquired by sensors. Particularly for Mobile Robot navigation in unknown environment, the type and number of sensors determines the data volume necessary to process and compose the image from the environment. Nevertheless, the excess of information imposes a great computational cost in data processing. Taking into account the temporal coherence between consecutive frames, a Discarding Criteria methodology based on Pearson's Correlation Coefficient (PCC) was proposed and applied as a Dynamic Power Management solution to a robotic visual-machine perception. In this context, this work proposes an environment observer method based on PCC that instead of processing all image pixels, it selects automatically only the regions-of-interest (ROI) and processes it in real time in order to perform a task: road detection and obstacle avoidance. This real-time visual perception system has been evaluated from real data obtained by two experimental platforms.**

I. Introduction

Lately, several applications for control of autonomous vehicles are being developed, and, in most cases, the machine vision is an important part of the set of sensors used for navigation. Some of these applications include: the aerial robots that offer great perspectives in many applications as search and rescue, real-time monitoring, high risk aerial missions, mapping, etc [1], [2]. Similarly, the development of Unmanned Aerial Vehicles (UAVs) has been of interest for military applications, however, one limitation is their maximum flight time; therefore they cannot carry large fuel payloads [3]. Future exploration of Mars requires long-endurance UAVs that use resources that are plentiful on Mars [4], [5], [6], [7]. Finally, for military or civil purposes, vehicular applications [8], [9], [10] have as objective the development of autonomous and semi-autonomous systems capable of traversing unrehearsed and off-road terrain, driving a car autonomously in an urban environment and also to help the driver in its driver task.

Manuscript received July 31, 2011.

Arthur de Miranda Neto is Ph.D. Student in Mechanical Engineering at the State University of Campinas – Brazil and in Information Technology and Systems at the University of Technology of Compiègne, France. Actually, he is researcher engineer at the Heudiasyc Lab CNRS UMR 6599.

Alessandro Corrêa Victorino is associate professor at the University of Technology of Compiègne – Heudiasyc Lab CNRS UMR 6599, France.

Isabelle Fantoni is researcher at the University of Technology of Compiègne – Heudiasyc Lab CNRS UMR 6599, France.

Douglas Eduardo Zampieri is associate professor of the Computational Mechanics Department, at the State University of Campinas, Brazil.

The perception is a common task to all cases previously presented, and an important factor is the variety and complexity of environments and situations. These real-time intelligent platform developments have a common issue: providing to the platform the capability of perceiving and interacting with its neighbour environment, managing power consumption, CPU usage, etc. Then, taking into account the temporal coherence between consecutive frames, this work proposes an environment observer method based on Pearson's Correlation Coefficient that observes if there are no significant changes in the environment, permitting that regions-of-interest (ROI) are automatically selected in order to perform a task: road detection and obstacle avoidance.

The Section II presents a review of previous works. The Section III introduces the Pearson's Correlation Coefficient, followed by the Discarding Criteria method in Section IV. The Automatic Regions-of-Interest (ROI) Selection is presented in the Section V. The results and conclusions are given in Section VI and VII.

II. Related Works

A. Sensor Perception

Environment perception is a major issue in autonomous vehicles. It uses many types of sensors [8], [9], including ultrasonic sensors, laser rangefinders, radar, cameras, etc. However, when incorporating several types of sensors, there is an increase of autonomy and "intelligence" degrees, especially in relation to navigation in unknown environments. In contrast, the type and quantity of sensors determine the volume of data for processing that requires, in most cases, a high computational cost. For unstructured environments, the scenario for study is dynamic, with several elements in motion. Thus, running a semi- or autonomous system involves carrying out complex, and non-deterministic operations in real time.

Moreover, a real-time system must satisfy explicit response-time constraints, including failure. This system is one whose logical correctness is based on both the correctness of the outputs and their timeliness [11]. Furthermore, there is a considerable complexity in the sense that correctness not only depends on the logical ordering of events of the systems, but also on the relative timing between them [12].

Aware that in the majority of the semi- and autonomous navigation systems, the machine-vision system is working

together with other sensors, added to its low cost, this paper proposed a monocular vision-based sensor. Because it uses simple techniques and fast algorithms, the system is capable to achieve a good performance, where the compromise between processing time and images acquisition is fundamental.

Additionally, the vision-based sensors are defined as passive sensors and the image scanning is performed fast enough for Intelligent Transportation Systems [13]. Furthermore, on the safety front, the progressive safety systems will be developed through the manufacturing of an "intelligent bumper" peripheral to the vehicle in answering new features as: blind spot detection, frontal and lateral pre-crash, etc. The objective in terms of cost to fill ADAS functions has to be very lower than the current Adaptive Cruise Control (500 Euros) [14].

B. Machine Vision

Autonomous robots can perform desired tasks in unstructured environments without continuous human guidance. An important variable is the state conditions in combination with environment events, because they may determine the system behavior.

In this way, Dynamic Power Management (DPM) is a design methodology for dynamically reconfiguring systems to provide the requested services and performance levels with a minimum number of active components or a minimum load on such components. For example, DPM and Real-Time Scheduling (RTS) techniques were presented in [15]. They were applied to reduce the power consumption of mobile robots. At the same time that scheduling is a key concept in computer multitasking and real-time operating system, the DPM dynamically adjusts power states of components adaptive to the task's need, reducing the power consumption without compromising system performance.

The machine vision, part of the embedded computers, is an important component of the set of sensors. Although extremely complex and highly demanding, thanks to the great deal of information it can deliver, it is a powerful means for sensing the environment and it has been widely employed to deal with a large number of tasks in the automotive field [13]. However, complex machine vision systems can lead to some losses due to the processing time.

A great amount of information would not necessarily lead to better decisions and could also harm the performance of the system, overloading it. Then, taking into account that it has been estimated that humans perceive visually about 90% of the environment information required for driving [13], it is not a bad idea to reduce information acquired by a vision system, in order to reduce processing time.

The method proposed here is based in an automatic image discarding criteria [16], [17], a low complexity and easy implemented solution. It improves the performance of a real-time system by choosing, in an automatic way, which images should be discarded and which ones should be treated at the visual perception system.

Furthermore, the fundamental premise for the applicability of DPM is that systems experience non-uniform workloads during operation time. A second assumption is that it is possible to predict, with a certain degree of confidence, the fluctuations of workload [18]. In this case, a simple DPM method shuts down a component when it is idle and it is essentially a prediction problem [15]. Thus, according to [18], the rationale in all predictive techniques is that of exploiting the correlation between the past history of the workload and its near future in order to make reliable predictions about future events.

III. PEARSON'S CORRELATION COEFFICIENT (PCC)

According to [19], an empirical and theoretical development that defined regression and correlation as statistical topics were presented by Sir Francis Galton in 1885. In 1895, Karl Pearson published the Pearson's Correlation Coefficient (PCC) [20]. The Pearson's method is widely used in statistical analysis, pattern recognition and image processing. Applications on the latter include comparing two images for image registration purposes, disparity measurement, etc [21]. It is described in (1):

$$r_1 = \frac{\sum_i (x_i - x_m)(y_i - y_m)}{\sqrt{\sum_i (x_i - x_m)^2}\sqrt{\sum_i (y_i - y_m)^2}} \quad (1)$$

where x_i is the intensity of the i^{th} pixel in image 1, y_i is the intensity of the i^{th} pixel in image 2, x_m is the mean intensity of image 1, and y_m is the mean intensity of image 2. The PCC threshold, r_1, has value 1 if the two images are identical, 0 if they are completely uncorrelated, and –1 if they are completely anti-correlated, for example, if one image is the negative of the other.

IV. DISCARDING CRITERIA

The discarding criteria was presented in [16] as a simple solution to improve the performance of a real-time navigation system by choosing, in an automatic way, which images should be discarded and which ones should be treated at the visual perception system. It was a new approach to the Pearson's Correlation Coefficient (PCC).

In Fig. 1, basically, if the PCC indicates that there is a high correlation between a reference frame and another new frame acquired, the new frame is discarded without being processed, Fig. 1 (c). In this case, some logical components may be shut down to save processor energy consumption, and/or to make the CPU available for running concurrent processes (the system can repeat a last valid command). Otherwise, the frame is processed and it is set as the new reference frame for the subsequent frame. For all cases

presented in this paper a threshold is chosen in an empirical way, as explained next.

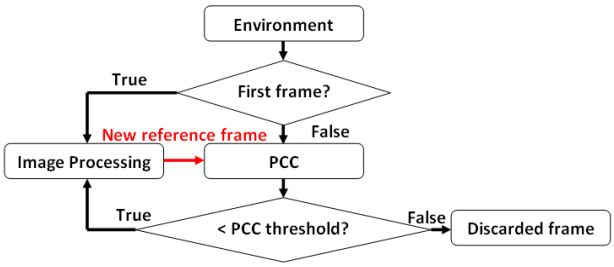

Fig. 1 – Discarding criteria [16].

Whereas the main problem that has to be faced when real-time imaging is concerned and which is intrinsic to the processing of images is the large amount of data [13], a logical dynamic optimization methodology based on Pearson's Correlation Coefficient (PCC) was introduced in [22]. To better understand this proposal, the Fig. 2 presents the accumulated time of a hypothetical image processing time (15ms) versus the gain obtained by using the discarding criteria, which could allow significant savings in CPU power consumption. In desert context were discarded 470 of 530 frames, whilst in off-road context were discarded 5595 of 6740 frames. For these two cases, the discarding rate remains over 80%.

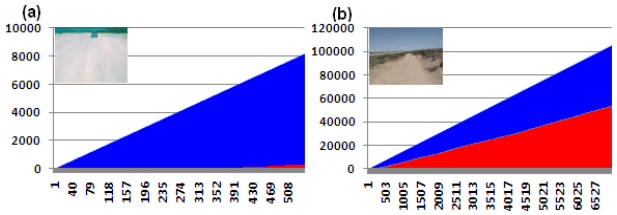

Fig. 2 – (a) Desert video [23]; (b) Off-road video [23]; In blue: the cumulative impact computations (ms) without the discarding criteria; In red: the cumulative computations (ms) by using the discarding criteria.

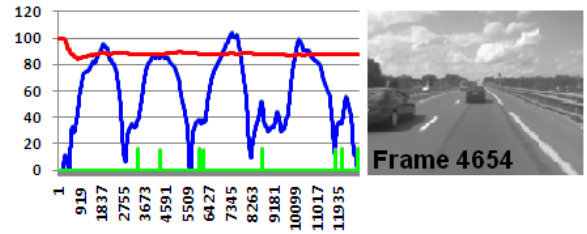

Fig. 3 – Real environment: Red line: discarding rate; Blue line: the vehicle speed; Green line: computational time (ms).

However, this discarding rate is not dependent on the video sequence or image size, but on the obstacles / objects influence. As shown in Fig. 3, it is also important to notice that there is no diffeomorphism between the robot speed and the PCC variation, because if there are no changes between consecutive frames, the PCC threshold remains static. In this case, the isomorphism cannot be guaranteed and it ensures more efficiency for our proposal. In real, dynamic and unknown environments, this rate remains over 65%. For these examples, the PCC threshold was fixed at 0.85.

V. Automatic Regions-of-Interest (ROI) Selection

According to the Pearson's correlation, in a certain analysis window (pair of frames), if the obstacle/object occupies a big portion of the scene, the PCC threshold tends to be low. Conversely, if obstacle/object occupies a small portion of the frame, it means that it is away from the vehicle and the system will have time enough to react. Nevertheless, where are these interest points/pixels? Or, which pixels (ROI) of the pair of images contributed most to the Pearson's coefficient computed? Which of them really need to be reprocessed (or resent to a server)?

Right after the Pearson's correlation in (1), it has x_m and y_m, respectively: the mean intensities of images 1 and 2, i.e. r_{1Xm} and r_{1Ym}.

From these two values, it begins again the process's correlation in (2), where for each pair of pixels analyzed, the only possible result is: [-1 or +1]. That is, all pixels with intensities below these means will be candidates for interest points. The Fig. 4 (c) and (f) present this process, where the red pixels (ROI) represent $r_2 = -1$.

$$r_2 = \frac{\sum_i (x_i - r_{1Xm})(y_i - r_{1Ym})}{\sqrt{\sum_i (x_i - r_{1Xm})^2}\sqrt{\sum_i (y_i - r_{1Ym})^2}} = \begin{cases} -1 \\ or \\ +1 \end{cases} \quad (2)$$

where x_i is the intensity of the i^{th} pixel in image 1, y_i is the intensity of the i^{th} pixel in image 2, r_{1Xm} and r_{1Ym} were obtained in (1).

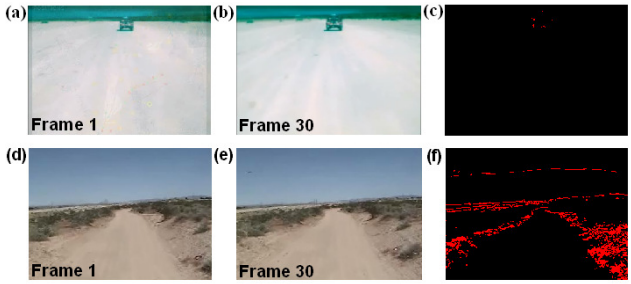

Fig. 4 – (a) and (b) are frames of the desert video [23]; (d) and (e) are frames of the off-road video [23]; (c) and (f) present the process's correlation in (2), where the red pixels (ROI) represent $r_2 = -1$.

A. *Road detection*

Different techniques on automatic and semi-automatic road extraction methods are proposed in the literature. With respect to these specific tasks, a road detection method based

on Otsu thresholding algorithm was proposed in [24], [25].

As shown in Fig. 1, the road detection process (imaging processing) is performed only when the PCC indicates that there is a low correlation between the reference frame and the current frame. Otherwise, the current frame is discarded without being processed. When an image is discarded, the system keeps the previous segmentation result, which is linked to an Otsu threshold. This stored threshold represents the navigable area. Consequently, in order to further improve the navigable area detection, for each discarded image, in Fig. 1, it classifies only the interest pixels (ROI) obtained in (2) from the last stored Otsu threshold. As an example, Fig. 5 (d) presents the interest pixels from the correlation between the Fig. 5 (a) and (b), where the white pixels (ROI) represent $r_2 = -1$. In Fig. 5 (e), these interest pixels are classified as navigable area in blue.

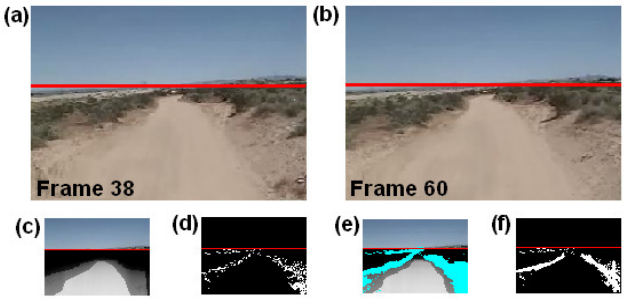

Fig. 5 – (a) and (b) are frames of the off-road video [23]; (c) the road detection process result; (d) the interest pixels (white pixels); (e) the interest pixels are classified as navigable area in blue; (f) line detection using Hough transform from the interest pixels (ROI) in Fig. 5 (d). The horizontal red lines represent the horizon detection process [25].

B. *Identifying the limits (boundaries) of the road*

In order to identify the limits of the road (which includes the obstacles), many research works proposing methods to detect road boundary. As an example, the Canny edge detector [26] can be employed as input of Hough transform [27] due to its robust performance and accurate edge localization. Nevertheless, to demonstrate another application for the proposed method here, Fig. 5 (f) presents the line detection using Hough transform from the Fig. 5 (d), where the white pixels represent $r_2 = -1$.

C. *Obstacle avoidance*

According to [28], the robots enter in the military context especially when it is necessary to reduce human exposure to hazardous situations. Many of these robotic missions can be observed, among them, as shown in Fig. 6 (d), an Improvised Explosive Device (IED) detonation. In this context, obstacle avoidance is a robotic discipline that includes reactive control in real time, i.e. reactive obstacle avoidance.

In this way, as discussed earlier, in order to make reliable predictions about future events, a predictive technique explores the correlation between the past history of the workload and its near future [18]. On the other hand, the Pearson's method explores regression and correlation aspects. Then, in order to reduce the risk of collision, for the obstacle avoidance task, it uses a PCC threshold equal to 0.65, which put in evidence the past history properties. In a computational process running in parallel to what was discussed in section V-A, for each frame processed, evidencing the past history properties, another old Otsu threshold is also stored. Besides the results presented in the Fig. 6, this procedure also allows a greater level of security, especially when the camera does not "see" the navigation area (i.e. in front of a wall), as will be shown in next section.

Therefore, for each discarded image, in Fig. 1, it classifies only the interest pixels (ROI) obtained in (2) from the last Otsu threshold obtained by a road detection algorithm (reference frame). Fig. 6 (c) and (f) represent the interest pixels classified as obstacle, where the white pixels (ROI) represent $r_2 = -1$. As shown in Fig. 6 (b) and (e), the interest pixels are classified as obstacle in yellow.

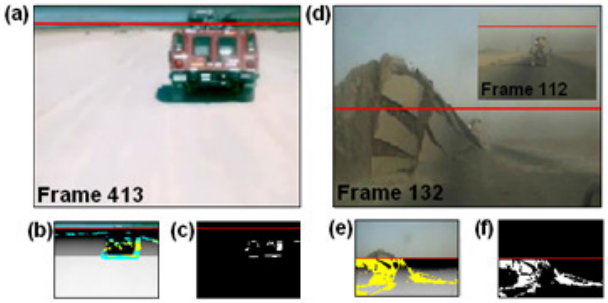

Fig. 6 – (a) is a frame of the off-road video [23]; (d) Improvised Explosive Device example; (b) and (e): the interest pixels are classified as navigable area in blue; (b) and (e): the interest pixels classified as obstacle in yellow. The horizontal red lines represent the horizon detection process [25].

VI. Experimental Results

Besides the experimental DARPA test-banks [23], this section presents results on real, dynamic and unknown environments, and they were obtained using two experimental vehicles, from a moving vehicle with a Sony DFW-VL500 camera. In order to reduce the number of data, it includes a resolution reduction of image to 160x120 pixels.

From displacements on the outskirts of the Heudiasyc Laboratory in France, the test-bank presented in the Fig. 7, 9 and 10 contains images recorded using the Carmen vehicle shown in Fig. 11 (a). The data were collected while a driver was driving the vehicle. Results for two different types of image texture (road surfaces) were selected and its results are presented in the Fig. 7 (b) and (e).

The next cases present autonomous displacements at Renato Archer IT Center (CTI) in Brazil. This stage of

testing evaluates the proposed algorithm at low speed on real-time conditions using the vehicle VERO shown in Fig. 11 (b). The VERO platform is equipped with SICK LMS and Hokuyo UTM30 outdoor laser scanners, GPS receiver, a monocular camera, and a CAN-bus interface which grants access to encoder data for the four wheels and steering, and allows commands to be sent to two independent motors driving the rear wheels and to control the steering angle. In the Fig. 8 (b) and (e), the trajectory control system had a single goal: to keep the robot in the center of the navigable path based on the mass of center. Fig. 8 (d) shows the task execution to go through a gate in off-road context. Fig. 8 (c) and (f) present the line detection using Hough transform from navigable area pixels. Two types of image texture (road surfaces) also were selected and its results are presented in Fig. 8 (b) and (e).

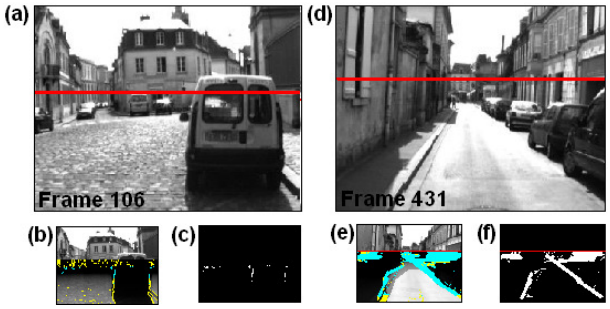

Fig. 7 – (a) and (d) are frames in real environments; (b) and (e): the interest pixels are classified as navigable area in blue; (b) and (e): the interest pixels are classified as obstacle in yellow; (c) and (f): line detection using Hough transform from navigable area pixels. The horizontal red lines represent the horizon detection process [25].

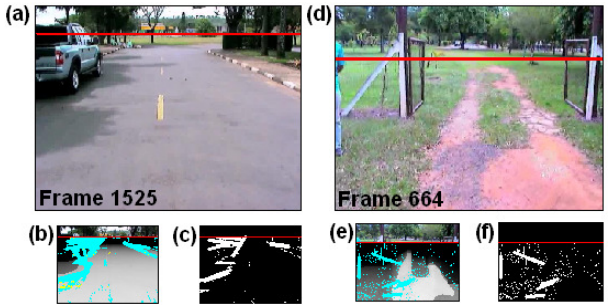

Fig. 8 – (a) and (d) are frames in real environments; (b) and (e): the interest pixels are classified as navigable area in blue; (b) and (e): the interest pixels are classified as obstacle in yellow; (c) and (f): line detection using Hough transform from navigable area pixels. The horizontal red lines represent the horizon detection process [25].

As expected, in grass areas, on the parallelepiped streets or where an excessive noise is observed, the efficiency of the method decreases considerably, what can be improved with the application of a smoothing filter, and/or from region-merging algorithm that mainly aims to represent homogeneous regions.

As shown in Fig. 9, it is not expected that a single camera provides all needed information to the safe navigation system to take decisions on routes. However, following what was presented in section VI-C: Obstacle avoidance, the new results in front of walls are presented in Fig. 10.

A video showing the application of this method is available in [29].

Fig. 9 – (a) Original image (in front of a wall) and its road detection result in (c); (b) Canny edge detection result.

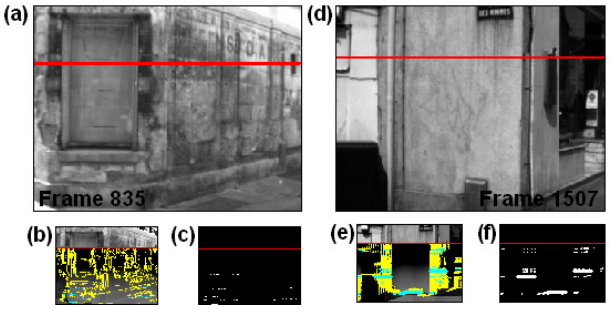

Fig. 10 – (a) and (d) are frames in real environments; (b) and (e): the interest pixels are classified as navigable area in blue; (b) and (e): the interest pixels are classified as obstacle in yellow; (f) and (i): line detection using Hough transform from navigable area pixels. The horizontal red lines represent the horizon detection process [25].

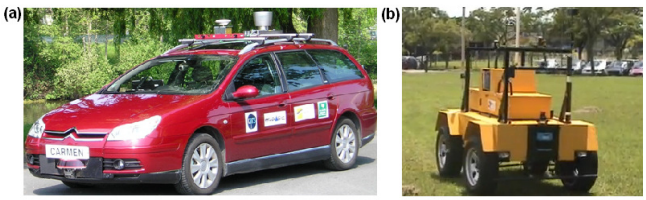

Fig. 11 – The experimental vehicles: (a) Carmen vehicle at Heudiasyc Laboratory in Compiegne, France; (b) Autonomous vehicle (VERO) at Renato Archer IT Center (CTI) in Campinas, Brazil.

VII. Conclusion

This work proposes a real-time machine vision algorithm based on monocular vision. It is important to notice that this algorithm is not based on previous knowledge of the environment (lane shape, geometric inference, etc) neither camera calibration. A remarkable characteristic of methodology presented in this work is its independence of the image acquiring system and of the robot itself. The same implementation works in different mobile robots, with

different embedded vision systems, without the need of adjusting parameters. Moreover, this visual-observer methodology may be extended to other sensors and components. Future work would be also focused to provide ground truth measurements from a front mounted radar and/or LIDAR system.

ACKNOWLEDGMENT

The authors wish to thank Dr. Luiz Gustavo Bizarro Mirisola, Dr. Samuel S. Bueno, Dr. Josué Jr. G. Ramos, Mr. Hélio Azevedo and Mr. Gerald Dherbomez for their kind attention to our work, for the useful discussions and support in data acquisition. This work was supported in part by French National Research Agency / ANR Percoive Project.

REFERENCES

[1] F. Bonin-Font, A. Ortiz, G. Oliver, (2008), "Visual Navigation for Mobile Robots: A Survey", Journal of Intelligent and Robotic Systems, 53, 3, 263-296, doi: 10.1007/s10846-008-9235-4

[2] B. Kim, P. Hubbard, D. Necsulescu, (2003), "Swarming Unmanned Aerial Vehicles: Concept Development and Experimentation, A State of the Art Review on Flight and Mission Control", DRDC-OTTAWA-TM-2003-176; Technical Memorandum.

[3] S. R. Anton, D.J. Inman, (2008), "Energy Harvesting for Unmanned Aerial Vehicles", In: Proceeding of SPIE.

[4] A. T. Klesh and P. T. Kabamba, (2009), "Solar-Powered Aircraft: Energy-Optimal Path Planning and Perpetual Endurance", Journal of Guidance, Control, and Dynamics.

[5] The Vision for Space Exploration, NASA, Feb. 2004, http://www.nasa.gov/pdf/55583main_vision_space_exploration2.pdf [retrieved 29 Nov. 2010].

[6] Energetically Autonomous Tactical Robot, (2009), DARPA Contract W31P4Q-08-C-0292.

[7] R. Finkelstein, Robotic Technology Inc, (2009), "Energetically Autonomous Tactical Robot and Associated Methodology of Operation", Patent Application number: 12/612,489, Publication number: US 2010/0155156 A1.

[8] S. Thrun, et al. (2006), "Stanley, the robot that won the DARPA Grand Challenge", Journal of Robotic Systems, Volume 23 , Issue 9, DARPA Grand Challenge, 661-692, ISSN:0741-2223, doi=10.1002/rob.v23:9

[9] Team Berlin (2007), Spirit of Berlin: An Autonomous Car for the DARPA Urban Challenge Hardware and Software Architecture, http://www.darpa.mil/grandchallenge/TechPapers/Team_Berlin.pdf [retrieved 02 Dec. 2010].

[10] O. Gietelink, J. Ploeg, B. De Schutter, and M. Verhaegen, (2006) "Development of advanced driver assistance systems with vehicle hardware-in-the-loop simulations," Vehicle System Dynamics, vol. 44, no. 7, pp. 569–590, doi=10.1080/00423110600563338

[11] P. Laplant, (2004), "Real-Time System Design and Analysis", IEEE Press, 3nd ed.

[12] P. Bouyer et al., (2010), "Quantitative analysis of real-time systems". Journal Communications of the ACM.

[13] M. Bertozzi. A. Broggi and A. Fascioli, (2000), "Vision-based intelligent vehicles: state of the art and perspectives", Robotics and Autonomous systems 32, 1-16, doi=10.1.1.36.3682

[14] Radio Spectrum Committee, European Commission, Public Document, Brussels, 5 July 2010, RSCOM10-35 http://ec.europa.eu/information_society/policy/ecomm/radio_spectrum/_document_storage/rsc/rsc32_public_docs/rscom10_35.pdf [retrieved 02 Dec. 2010].

[15] H. Y. L. C. Yongguo Mei, Yung-Hsiang Lu, (2005), "A case study of mobile robot's energy consumption and conservation techniques", Proceedings of the the IEEE International Conference on Advanced Robotics, ICAR 2005, pp. 492-497, doi=10.1109/ICAR.2005.1507454

[16] A. Miranda Neto, L. Rittner, N. Leite, D. E. Zampieri, R. Lotufo and A. Mendeleck, (2007), "Pearson's Correlation Coefficient for Discarding Redundant Information in Real Time Autonomous Navigation Systems", Proceedings of the 2007 IEEE Multi-conference on Systems and Control, doi: 10.1109/CCA.2007.4389268

[17] A. Miranda Neto, L. Rittner, N, Leite, D. E. Zampieri and A. C. Victorino, (2008), "Nondeterministic Criteria to Discard Redundant Information in Real Time Autonomous Navigation Systems based on Monocular Vision", ISIC Invited Paper, 2008 IEEE Multi-conference on Systems and Control, San Antonio, Texas, EUA, September 3-5, doi: 10.1109/ISIC.2008.4635955

[18] L. Benini, A. Bogliolo, and G. D. Micheli. (2000), "A Survey of Design Techniques for System-Level Dynamic Power Management", IEEE Transactions on Very Large Scale Integration Systems, 8(3):299-316, doi=10.1109/92.845896

[19] J. L. Rodgers and W. A. Nicewander, (1988), "Thirteen Ways to Look at the Correlation Coefficient", The American Statistician, 42, 59-66.

[20] K. Pearson, (1895), Royal Society Proceedings, 58, 241.

[21] Y. K. Eugene and R.G. Johnston, "The Ineffectiveness of the Correlation Coefficient for Image Comparisons", Technical Report LA-UR-96-2474, Los Alamos, 1996.

[22] A. Miranda Neto, A. C. Victorino, I. Fantoni and D. E. Zampieri, (2011), "Real-Time Dynamic Power Management based on Pearson's Correlation Coefficient", Proceedings of the IEEE International Conference on Advanced Robotics, ICAR 2011, to appear.

[23] DARPA 2005. "DARPA Grand Challenge", http://www.darpa.mil/grandchallenge05/

[24] A. Miranda Neto and L. Rittner, (2006), "A Simple and Efficient Road Detection Algorithm for Real Time Autonomous Navigation based on Monocular Vision", Proceedings of the 2006 IEEE 3rd Latin American Robotics Symposium, doi=10.1109/LARS.2006.334325

[25] A. Miranda Neto, A. C. Victorino, I. Fantoni and D. E. Zampieri, (2011), "Robust Horizon Finding Algorithm for Real-Time Autonomous Navigation based on Monocular Vision", submitted to Proceedings of the IEEE Int. Conf. on Intelligent Transportation Systems, ITSC 2011, to appear.

[26] J. F. Canny, (1986), "A computational approach to edge detection". IEEE Trans. Pattern Anal. Machine Intell. 8 (6), 679–698, doi=10.1109/TPAMI.1986.4767851

[27] D. Ballard, (1981), "Generalized Hough transform to detect arbitrary shapes", IEEE Trans. Pattern Anal. Machine Intell. 13 (2), 111–122.

[28] R. Chatila, (2010), "Dual research: Issues in robotics", Oral presentation, Mission for Research and Innovation Scientific 2010. Directorate General of Armaments (DGA), Paris, France.

[29] http://www.youtube.com/watch?v=VcUQVC1F8Xw